Published in final edited form as:
Cell Host Microbe. 2014 June 11; 15(6): 768–778. doi:10.1016/j.chom.2014.05.012.

Porphyromonas gingivalis manipulates complement and TLR signaling to uncouple bacterial clearance from inflammation and promote dysbiosis

Tomoki Maekawa[1,7], **Jennifer L. Krauss**[2,7,8], **Toshiharu Abe**[1], **Ravi Jotwani**[2], **Martha Triantafilou**[3], **Kathy Triantafilou**[3], **Ahmed Hashim**[4], **Shifra Hoch**[5], **Michael A. Curtis**[4], **Gabriel Nussbaum**[5], **John D. Lambris**[6], and **George Hajishengallis**[1,*]

[1]University of Pennsylvania, School of Dental Medicine, Department of Microbiology, Philadelphia, PA 19104, USA

[2]University of Louisville, Center for Oral Health and Systemic Disease, Louisville, KY 40292, USA

[3]Cardiff University School of Medicine, Institute of Infection and Immunity, Cardiff CF14 4XN, UK

[4]Queen Mary University of London, Centre for Immunology and Infectious Disease, Blizard Institute, Barts and The London School of Medicine and Dentistry, London E1 2AT, UK

[5]Hebrew University, Hadassah Dental School, Jerusalem 12272, Israel

[6]University of Pennsylvania, Perelman School of Medicine, Department of Pathology and Laboratory Medicine, Philadelphia, PA 19104, USA

SUMMARY

Certain low-abundance bacterial species, such as the periodontitis-associated oral bacterium *Porphyromonas gingivalis* can subvert host immunity to remodel a normally symbiotic microbiota into a dysbiotic, disease-provoking state. However, such pathogens also exploit inflammation to thrive in dysbiotic conditions. How these bacteria evade immunity while maintaining inflammation is unclear. As previously reported, *P. gingivalis* remodels the oral microbiota into a dysbiotic state by exploiting complement. Now we show that in neutrophils *P. gingivalis* disarms a host-protective TLR2-MyD88 pathway via proteasomal degradation of MyD88, whereas it activates an alternate TLR2-Mal-PI3K pathway. This alternate TLR2-Mal-PI3K pathway blocks

*Correspondence: geoh@upenn.edu.
[7]Co-first author.
[8]Present address: Department of Pathology, Washington University School of Medicine, St. Louis, MO 63110.

AUTHOR CONTRIBUTIONS

Co-first authors T.M. and J.L.K. performed most of the *in vivo* and *in vitro* assays and analyzed the data. T.A., R.J., M.T., K.T., A.H., S.H. performed research and data analysis. M.A.C. and G.N. performed data analysis and discussed the proposed model with G.H. J.D.L. and G.H. conceived of and designed research. GH supervised research and wrote the paper. All authors approved the final manuscript.

The authors declare no financial conflicts of interest.

phagocytosis, provides 'bystander' protection to otherwise susceptible bacteria, and promotes dysbiotic inflammation *in vivo*. This mechanism to disengage bacterial clearance from inflammation required an intimate crosstalk between TLR2 and the complement receptor C5aR, and can contribute to the persistence of microbial communities that drive dysbiotic diseases.

INTRODUCTION

Dysbiosis, a state characterized by imbalances in the relative abundance or influence of microbial species within an ecosystem, is emerging as a potential trigger of mucosal inflammatory disorders, such as inflammatory bowel disease, colorectal cancer, bacterial vaginosis, and periodontitis (Eloe-Fadrosh and Rasko, 2013; Hajishengallis et al., 2012). The mechanisms leading to dysbiosis are poorly understood and hence under intensive investigation. In this regard, the keystone-pathogen hypothesis holds that certain low-abundance pathogens can subvert host immunity in ways that favor the remodeling of a normally symbiotic microbiota into a dysbiotic and disease-provoking state (Hajishengallis et al., 2012; Stecher et al., 2013).

For instance, the oral asaccharolytic bacterium *Porphyromonas gingivalis* (Pg) fails to cause periodontitis in germ-free mice despite colonizing this host; however, in conventional mice, Pg transforms the periodontal microbiota into a dysbiotic community and co-opts it to instigate destructive inflammation (Hajishengallis et al., 2011). In contrast, C5a receptor (C5aR; CD88)-deficient mice are protected from Pg-induced dysbiosis and periodontitis (Hajishengallis et al., 2011). The ability of Pg to instigate inflammatory disease through community-wide supportive effects, while being a low-abundance constituent of periodontitis-associated biofilms in humans and animal models (Abusleme et al., 2013; Hajishengallis et al., 2011), has prompted its designation as a keystone pathogen (Hajishengallis et al., 2012).

Organisms involved in dysbiotic diseases are burdened with the challenge of evading host immunity in an inflammatory environment. In this respect, we hypothesized that the survival and persistence of Pg is crucially dependent upon its capacity to selectively manipulate the host response in ways that would suppress killing mechanisms but not inflammation. This is because inflammation actually serves the nutritional needs of asaccharolytic dysbiotic communities through the release of tissue breakdown products including peptides and heme-containing compounds (Hajishengallis, 2014). Therefore, although immunosuppression is a common immune evasion strategy of many pathogens (Cyktor and Turner, 2011), it should not be a viable option for pathobionts that thrive on inflammation. However, the molecular mechanism(s) by which immune-subversive bacteria such as Pg can selectively inhibit immune elimination without suppressing inflammation have remained obscure. Since neutrophils are heavily involved in the initiation and progression of human periodontitis and comprise ≥95% of total leukocytes in periodontal pockets where they constantly encounter Pg (Hajishengallis and Hajishengallis, 2014; Nussbaum and Shapira, 2011), we addressed this issue in the context of Pg-neutrophil interactions *in vitro* and *in vivo*. Our study dissected how *P. gingivalis* subverts complement and Toll-like receptor (TLR) signaling to inhibit bacterial killing while preserving inflammation and promoting dysbiosis *in vivo*.

RESULTS

Pg inhibits the killing but not the proinflammatory activity of neutrophils *in vivo*

The ability of Pg to persist and cause dysbiosis and periodontitis in mice requires intact C5aR signaling (Abe et al., 2012; Hajishengallis et al., 2011). Since neutrophils constitute the overwhelming majority of professional phagocytes recruited to periodontal pockets, we hypothesized that Pg exploits C5aR to inhibit neutrophil killing but not neutrophil-mediated inflammation. To address this hypothesis in a quantitative way, we used the mouse chamber model (Burns et al., 2010; Mydel et al., 2006). This model involves injectable inoculation of bacteria into the lumen of a subcutaneously implanted titanium-coil chamber, thereby allowing quantitative assessment of bacterial interactions with recruited neutrophils (>97% of recruited leukocytes; Figure 1A). Since innate pattern recognition of Pg is predominantly mediated by TLR2 (Burns et al., 2010), which synergizes with C5aR in periodontal inflammation (Abe et al., 2012), we examined the interactions of Pg with both C5aR and TLR2 using knockout mice or specific inhibitors.

At 2h post-inoculation with Pg, chamber fluid aspirated from mice lacking C5aR (*C5ar*$^{-/-}$) or TLR2 (*Tlr2*$^{-/-}$), or from wild-type (WT) mice treated with C5aR antagonist (C5aRA) or anti-TLR2, contained significantly lower Pg viable counts (CFU) as compared with corresponding controls (*i.e.*, WT mice that were left untreated or treated with control compounds) (Figure 1B). In contrast, Pg CFU counts recovered from the chambers of mice lacking complement receptor 3 (CR3; *CD11b*$^{-/-}$) did not differ from those recovered from WT controls (Figure 1B). These data suggested that both C5aR and TLR2 are required for enhanced Pg survival in the chambers. Consistent with this, a gingipain-deficient isogenic mutant (KDP128), which cannot generate C5a to activate C5aR (Liang et al., 2011), was extremely susceptible to killing unless C5a was added exogenously resulting in decreased phagocytosis (Figure S1). Interestingly, despite their increased capacity to clear Pg, *C5ar*$^{-/-}$ mice and C5aRA-treated WT mice recruited lower numbers of neutrophils (typically 2.5 [±0.8] ×10^6) as compared to those in untreated WT mice (typically 1.0 [±0.3] ×10^7), whereas the recruitment of neutrophils in the chambers of *Tlr2*$^{-/-}$ mice and anti-TLR2-treated WT mice was not significantly affected compared with untreated WT controls (not shown). No Pg viable counts could be recovered from blood or internal organs (spleen, liver, lungs, and kidney) from WT or knockout mice; similarly, quantitative real-time PCR of the *ISPg1* gene of Pg failed to detect Pg in those tissues.

Treatment of *Tlr2*$^{-/-}$ mice with C5aRA (or, conversely, treatment of *C5ar*$^{-/-}$ mice with anti-TLR2) had no further inhibitory effect on Pg viability compared to untreated *Tlr2*$^{-/-}$ (or *C5ar*$^{-/-}$) mice (Figure 1B). This finding and the observation that the survival of Pg is inhibited to the same extent regardless of which of the two receptors (C5aR or TLR2) is lacking or blocked collectively suggest that C5aR and TLR2 engage in cooperative crosstalk to prevent Pg killing. This C5aR/TLR2-dependent evasive mechanism is unlikely to involve generalized neutrophil immunosuppression, since the induction of proinflammatory cytokines in the chambers was higher when both C5aR and TLR2 were functional (WT mice) than when C5aR or TLR2 signaling was ablated genetically (*C5ar*$^{-/-}$ and *Tlr2*$^{-/-}$ mice) or pharmacologically (C5aRA-treated and anti-TLR2-treated WT mice) (Figure 1C).

In contrast to Pg, the periodontal and systemic pathogen *Fusobacterium nucleatum* (Hajishengallis and Lamont, 2012; Rubinstein et al., 2013) was susceptible to neutrophil killing in the chambers of WT mice (Figure 1D, **far left**). Intriguingly, the survival of *F. nucleatum* was remarkably enhanced by about 3 $\log_{10}$ units in co-infection experiments with Pg in WT but not in *C5ar*$^{-/-}$ or *Tlr2*$^{-/-}$ mice (Figure 1D). Therefore, Pg can rescue *F. nucleatum* in a C5aR- and TLR2-dependent manner.

Pg induces C5aR-TLR2 co-association in human neutrophils and inhibits their killing function

To test the potential human relevance of the C5aR/TLR2-dependent evasion mechanism of Pg in mice, we performed receptor blockade experiments in human neutrophils. The ability of human neutrophils to kill Pg was significantly enhanced by blocking C5aR or TLR2, but not other receptors such as CR3 or CXCR4 (Figure 2A), suggesting that intact C5aR and TLR2 signaling is required for maximal protection of Pg against also human neutrophils. Unlike our previous findings with macrophages (Wang et al., 2010), the mechanism underlying immune evasion of neutrophils did not involve cAMP-dependent protein kinase A (PKA) signaling, since treatments with inhibitors of cAMP synthesis (SQ22536) or of PKA (PKI 6-22 or H89) failed to influence the capacity of neutrophils to kill Pg (Figure 2A).

Although C5a is produced endogenously in the cell-bacterial cultures by direct enzymatic action of the Pg gingipains on C5 (Liang et al., 2011; Wang et al., 2010), exogenous addition of extra C5a further inhibited neutrophil killing of Pg in a C5aR (CD88)-dependent manner (Figure 2B). On the other hand, exogenous C5a augmented the Pg-induced oxidative burst in a C5aR-dependent manner (Figure 2C), suggesting that the mechanism whereby Pg evades killing involves interference with a subset of neutrophil responses rather than immune paralysis.

Confocal microscopy of Pg-stimulated human neutrophils revealed colocalization of Pg with C5aR (Figure 2D), which came into molecular proximity with TLR2 (but not TLR5 or MHC Class I) in Pg-stimulated (but not resting) neutrophils, as shown by FRET (Figure 2E). This C5aR-TLR2 co-association probably takes place in lipid rafts, as there was significant energy transfer between these receptors and the lipid raft marker GM1 (Figure 2E). In summary, Pg interacts with and exploits C5aR and TLR2 in human neutrophils to enhance its survival. We next set out to dissect the evasive mechanism(s) acting downstream of C5aR and TLR2.

Pg-induced C5aR-TLR2 crosstalk leads to MyD88 degradation

Despite being a TLR2 signaling adaptor (O'Neill and Bowie, 2007), MyD88 is unlikely to contribute to immune evasion mediated by the Pg-induced C5aR-TLR2 crosstalk; indeed, MyD88 was shown to contribute to the clearance of Pg infection (Burns et al., 2010). Accordingly, Pg exhibited enhanced survival in the chambers of *Myd88*$^{-/-}$ mice as compared with WT mice (Figure 3A **far left**). We then investigated whether Pg can counteract MyD88 and thereby achieve increased protection against neutrophils. Strikingly, Pg caused time-dependent reduction in the levels of MyD88 protein but not mRNA (Figure

3B), suggesting that Pg causes MyD88 degradation at least *in vitro*. The ability of Pg to degrade MyD88 was completely reversed by C5aRA or anti-TLR2 (Figure 3C), suggesting that degradation is mediated by C5aR-TLR2 crosstalk. A TLR2 agonist, the synthetic lipopeptide Pam3CSK4, failed to induce MyD88 degradation (Figure 3B), suggesting that TLR2 activation by itself is not sufficient for this effect. However, Pam3CSK4 together with C5a did induce MyD88 degradation reproducing the phenotype of Pg-treated cells and confirming dependence on concomitant activation of TLR2 and C5aR for MyD88 degradation (Figure S2A). Moreover, Pg induced ubiquitination of MyD88, which correlated temporally with reduced MyD88 protein levels (Figure 3D). This observation suggested that the reduction in MyD88 protein levels was mediated by ubiquitin-proteasome degradation, a notion supported by the reversal of Pg-induced degradation of MyD88 by the proteasome inhibitor epoxomycin (Figure 3E). Pg caused C5aR- and TLR2-mediated and ubiquitin-proteasome–dependent degradation of MyD88 also in all-trans retinoic acid (ATRA)–differentiated HL-60 neutrophils (Figure S2 B-G), thus validating the use of these cells as a model of Pg exploitation of human neutrophils. Using a siRNA approach and ATRA–HL-60 cells, we have shown that Pg-induced ubiquitination and degradation of MyD88 requires the E3 ubiquitin ligase Smad ubiquitin regulatory factor 1 (Smurf1). Indeed, when Smurf1 protein expression was diminished by siRNA to Smurf1, the ability of Pg to degrade MyD88 was suppressed (Figure 3F). Consistently, diminished expression of Smurf1 due to specific siRNA treatment resulted in reduced ubiquitination of MyD88 in Pg-treated cells (Figure 3F). In contrast to Smurf1, other E3 ubiquitin ligases involved in the regulation of TLR signaling pathways (Triad3A and Pellino-1) were shown to not be involved in Pg-induced ubiquitination and degradation of MyD88 (Figure S2H). Our investigation of Smurf1 was prompted by our findings that transforming growth factor-β1 (TGF-β1), a cytokine shown to cause ubiquitin-proteasome degradation of MyD88 via Smurf1 (Lee et al., 2011), was induced in Pg-challenged neutrophils in a C5aR/TLR2-dependent manner (Figure S2I). Consistently, antibody-mediated neutralization of TGF-β abrogated the ability of Pg to ubiquitinate and degrade MyD88 (Figure 3G).

Importantly, Pg (but not Pam3CSK4) induced degradation of MyD88 also *in vivo*, as shown by examining neutrophils harvested from Pg-inoculated mouse chambers (Figure 3H). In contrast, *F. nucleatum*, which is susceptible to neutrophil killing in the chambers (Figure 1D), failed to induce MyD88 degradation (Figure 3H). Neutrophils purified from the bone marrow of *Myd88*$^{-/-}$ mice exhibited decreased killing activity against Pg compared to WT controls, which in turn were less potent in killing Pg than *Tlr2*$^{-/-}$ or *C5ar*$^{-/-}$ neutrophils (Figure 3I). Therefore, although MyD88 contributes to neutrophil control of Pg, the pathogen can counteract this host defense mechanism by inducing degradation of MyD88.

MyD88-independent activation of PI3K inhibits Pg phagocytosis and induces inflammation

The data in figures 1-3 show that Pg evades both mouse and human neutrophils through a common C5aR/TLR2-mediated mechanism that involves MyD88 degradation. Therefore, findings in the mouse chamber model are relevant to and predictive of findings in the human system of Pg-neutrophil interactions. We thus used the chamber model to obtain additional mechanistic insights on how Pg manipulates neutrophils *in vivo*. Although Pg exhibited enhanced survival in the genetic absence of MyD88, treatments with C5aRA or anti-TLR2

promoted the killing of Pg in the chambers of *Myd88*$^{-/-}$ mice and diminished its viable counts to levels similar to those seen in the chambers of *C5ar*$^{-/-}$ or *Tlr2*$^{-/-}$ mice (Figure 3A). This finding suggested that C5aR and TLR2 promote the survival of Pg also via MyD88-independent mechanism(s). In this regard, treatment of mice with the phosphatidylinositol-3-OH kinase (PI3K) inhibitor LY294002 (but not with the inactive analog LY303511) resulted in significant reduction of Pg CFU counts (Figure 4A) to levels comparable to those seen after inhibition of C5aR or TLR2 signaling (Figure 1B). The increased killing of Pg in the presence of LY294002 was not associated with changes in the numbers of recruited neutrophils (Figure 4B) and was attributed to promotion of phagocytosis (Figure 4C). In contrast, LY294002 had no significant effect on the phagocytosis of *F. nucleatum* (Figure S3A). C5aRA or anti-TLR2 treatment enhanced Pg phagocytosis *in vivo* (in the chambers; Figure 4C) and *in vitro* (in Pg-neutrophil cultures; Figure S3B) comparably to LY294002, suggesting that PI3K may be acting as an effector of a signaling crosstalk between C5aR and TLR2. Indeed, maximal activation of PI3K (Tyr phosphorylation of its p85 regulatory subunit) by Pg in purified mouse neutrophils required the presence of both C5aR and TLR2, although it was essentially independent of MyD88 (Figure 4D, **left**). Stimulation of neutrophils with both Pam3CSK4 and C5a caused considerably higher PI3K activation compared to each ligand alone, thereby reproducing the phenotype obtained by Pg and confirming dependence on TLR2 and C5aR for synergistic PI3K activation (Figure 4D, **right**). Consistent with the notion that PI3K is an effector of the subversive C5aR-TLR2 crosstalk, the capacity of Pg to protect *F. nucleatum* against neutrophil killing in co-infection experiments was abrogated in the presence of LY294002 (but not LY303511) (Figure 4E), as seen earlier in the absence of C5aR or TLR2 signaling (Figure 1D).

Given that the *in vivo* host response to Pg is MyD88-independent (Burns et al., 2010), we hypothesized that PI3K acts downstream of C5aR and TLR2 to promote inflammation. We therefore assessed induction of proinflammatory cytokines (IL-1β, IL-6, and TNF) in the chambers of Pg-inoculated WT mice in the presence of LY294002 or LY303511 control. LY294002 (but not LY303511) inhibited the inflammatory responses, thereby implicating PI3K in the process (Figure 4F). A similar but less pronounced PI3K-depedent effect was observed when Pam3CSK4 was injected in the chambers in lieu of Pg (Figure S3C).

The mechanism by which the C5aR-TLR2-PI3K pathway inhibited Pg phagocytosis involved inhibition of actin polymerization, a process required for phagocytosis. Indeed, C5aRA, anti-TLR2, and LY294002 (but not their respective controls) promoted Pg-induced actin polymerization (Figure 4G), suggesting that Pg suppresses actin polymerization when the C5aR-TLR2-PI3K pathway remains functional. Pg also suppressed the activation of RhoA (Figure 4H and Figure S3D), a key regulator of actin polymerization (Wiedemann et al., 2006). The ability of Pg to prevent RhoA activation was counteracted by C5aRA, anti-TLR2, and LY294002 (but not their respective controls) as shown by an ELISA-based assay that measures the levels of GTP-loaded RhoA (Figure 4H) or a related pull-down assay (Figure S3D). Taken together, Pg inhibits phagocytosis by exploiting C5aR/TLR2-dependent PI3K signaling which suppresses RhoA activation and actin polymerization. Consistent with *in vivo* mouse data (Figure 4F), LY294002 inhibited inflammatory cytokine

responses by Pg-stimulated human neutrophils, as did treatments with C5aRA or anti-TLR2 (Figure 4I). In summary, Pg escapes phagocytic killing and induces inflammatory responses in neutrophils by activating PI3K in a way dependent upon C5aR and TLR2 but not MyD88.

PI3K mediates periodontal dysbiosis and inflammation

The ability of Pg to cause dysbiosis and periodontitis requires intact C5aR signaling (Abe et al., 2012; Hajishengallis et al., 2011). In contrast to WT Pg, the KDP128 mutant that lacks C5a-generating capacity failed to cause changes to the amount and composition of the oral microbiota (Figure S4). Interestingly, compositional shifts in the murine oral microbiota are not necessarily associated with periodontal inflammation, unless they are accompanied by a significant increase in the bacteria load (Eskan et al., 2012). To further characterize host signaling pathways involved in Pg-induced elevation of the total microbiota counts and periodontal inflammation, Pg-colonized mice were locally microinjected in the gingiva with various inhibitors and their effects on the microbiota and host response were assessed two days later. The main purpose was to determine the role of PI3K in dysbiotic inflammation in relation to C5aR and TLR2. We found that LY294002 (but not LY303511) almost eliminated Pg from the periodontal tissue (Pg numbers were decreased by $\approx$1.5 $\log_{10}$ units corresponding to 97% reduction) and reversed the increase in the total microbial load induced by Pg colonization; these effects were similar to those of C5aRA and anti-TLR2 (but not anti-TLR4 which had no effect) (Figure 5A). Moreover, pharmacological inhibition of PI3K with LY294002 (but not with LY303511 control) inhibited Pg-induced expression of inflammatory cytokines in the periodontal tissue (at both the mRNA and protein levels; Figure 5 B and C, respectively), as seen earlier after genetic or pharmacological ablation of C5aR or TLR2 (Abe et al., 2012; Hajishengallis et al., 2011; Liang et al., 2011). Taken together, our findings are consistent with the notion that PI3K is an effector of the subversive C5aR-TLR2 crosstalk that protects Pg and contributes to dysbiotic inflammation.

Mal is a component of the C5aR-TLR2 subversive pathway acting upstream of PI3K

MyD88-adapter-like (Mal), another adaptor molecule involved in TLR2 signaling, has been reported to bridge MyD88 to the receptor complex but it can also interact with and activate PI3K (Honda et al., 2012; Kagan and Medzhitov, 2006; O'Neill and Bowie, 2007; Santos-Sierra et al., 2009). Therefore, it could not be predicted whether Mal would have a host-protective role similar to MyD88, or whether it would cooperate with the C5aR-TLR2-PI3K subversive pathway. To determine the role of Mal in neutrophil killing of Pg, we performed siRNA-mediated Mal gene silencing in ATRA-differentiated HL-60 neutrophils. Treatment with siRNA to Mal promoted the killing of Pg similarly to C5aRA, anti-TLR2, or LY294002, whereas siRNA to MyD88 inhibited the killing of Pg relative to untreated cells or cells treated with control siRNA (Figure 6A). Moreover, siRNA to Mal promoted Pg phagocytosis (Figure 6B) further suggesting that Mal is a component of the immunoevasive pathway of Pg. Treatments of ATRA–HL-60 cells with siRNA to Mal also inhibited Pg-induced activation of PI3K (Figure 6C) and induction of proinflammatory cytokines (Figure 6D), suggesting that Mal acts upstream of PI3K. The immunoevasive and proinflammatory role of Mal was confirmed by similar findings in mouse neutrophils treated with a cell-permeable Mal inhibitor peptide (Figure S5 A-D), and also by genetic evidence using WT and Mal-deficient neutrophils in the same assays (Figure S5 E-I). Moreover, *MyD88*$^{-/-}$

neutrophils responded to Pg (monitored by TNF production) in a strictly PI3K-dependent manner, whereas *MyD88*$^{-/-}$ macrophages failed to respond at all (Figure S5K). These data further support the existence of a Pg-induced MyD88-independent proinflammatory PI3K pathway in neutrophils. Co-immunoprecipitation analysis showed that PI3K associated with both TLR2 and Mal in Pg-activated ATRA–HL-60 cells or primary human neutrophils (Figure 6E). In summary, Mal is an essential component of the TLR2-PI3K subversive pathway that inhibits Pg phagocytosis and killing while promoting inflammatory responses.

DISCUSSION

Although neutrophils in the periodontal pockets of patients with chronic periodontitis form a ‘defense wall’ against the bacteria, they largely fail to control bacterial growth and prevent dysbiosis despite being viable and capable of immune responses (Ryder, 2010). In fact, periodontitis patients have a greater number of and longer-lived neutrophils in the oral tissues compared with healthy controls (Lakschevitz et al., 2013). Our findings provide molecular explanation for the inability of human (and mouse) neutrophils to control periodontal bacteria and prevent dysbiotic inflammation. Specifically, we showed that Pg instigates a crosstalk between C5aR and TLR2 to disarm and disassociate a host-protective TLR2–MyD88 pathway from a proinflammatory and immune-evasive TLR2–Mal–PI3K pathway (Figure 7). Neutrophils exposed to Pg were impaired also in the clearance of bystander bacterial species as long as Pg had access to functional C5aR and TLR2, consistent with the capacity of Pg to elevate the total microbiota counts in periodontal tissue with intact C5aR and TLR2 signaling.

The subtle manipulation of the human neutrophil response by Pg is probably the result of coevolution with the host, in which Pg could persist only if its ability to evade killing would not interfere with the inflammatory response. This is because periodontal bacteria including Pg depend critically on an inflammatory environment to obtain nutrients in the form of tissue-breakdown products (*e.g.*, peptides and heme-containing compounds) (Hajishengallis and Lamont, 2014). Such bacteria are therefore “inflammo-philic” (from the Greek suffix *philic* meaning attracted to or loving). Consistent with this concept, the bacterial biomass of human periodontitis-associated biofilms increases with increasing periodontal inflammation (Abusleme et al., 2013), and anti-inflammatory treatments in animal models suppress the periodontal bacterial load (Eskan et al., 2012; Hasturk et al., 2007; Moutsopoulos et al., 2014). This vital dependence on inflammation could account for the radically different behavior of Pg as compared with certain other major immune-evasive bacteria such as *Staphylococcus aureus*. Whereas Pg expresses virulence factors (gingipains) to proactively generate C5a and activate C5aR (Liang et al., 2011; Wang et al., 2010), *S. aureus* expresses a virulence factor (chemotaxis inhibitory protein) to block C5aR activation (de Haas et al., 2004). Moreover, *S. aureus* expresses a leukotoxin that targets and kills neutrophils (Reyes-Robles et al., 2013), whereas Pg manipulates but does not kill neutrophils. It could be speculated that inflammophilic pathobionts in diverse disease settings (*e.g.*, thriving in gut dysbiosis and implicated in inflammatory bowel disease (Stecher et al., 2013)) may use immune subversive strategies analogous to those of Pg.

TGF-β1 is a pluripotent cytokine with complex and context-dependent regulatory effects on inflammation (Wahl, 1994; Yang et al., 2010), including ubiquitination and negative regulation of MyD88 signaling (Lee et al., 2011; Naiki et al., 2005) as well as promotion of neutrophil recruitment and activation (Wahl, 1994). The augmented production of TGF-β1 by Pg-stimulated neutrophils in a C5aR/TLR2-dependent manner prompted us to hypothesize and show that this cytokine mediated the C5aR/TLR2-dependent ubiquitination and degradation of MyD88 via the E3 ubiquitin ligase Smurf1.

The mechanism by which MyD88 mediates neutrophil killing of Pg may not necessarily be related to MyD88-dependent transcriptional programs. The MyD88-IRAK4 pathway was shown to mediate TLR-triggered neutrophil exocytosis (Brzezinska et al., 2009) and to control bacterial killing (Suzuki et al., 2002). Further research is warranted to determine whether such mechanism also operates for the control of Pg. Although MyD88 also participates in the induction of the neutrophil oxidative burst (Miletic et al., 2007), this mechanism is unlikely to explain the antimicrobial effect of MyD88 against Pg. This is because Pg is quite resistant to oxidative burst killing by neutrophils (Hajishengallis et al., 2008; Mydel et al., 2006), although in gingival epithelial cells, where this bacterium can reside intracellularly, Pg inhibits the long-term production of reactive oxygen species despite an early activation of the oxidative response (Choi et al., 2013).

In stark contrast to MyD88, Mal acted as a critical component of an immune-evasive and proinflammatory pathway acting downstream of the C5aR-TLR2 crosstalk and upstream of PI3K (Figure 7). This MyD88-independent proinflammatory PI3K pathway could be activated by Pg in neutrophils but not macrophages. Although Mal can mediate MyD88-independent activation of PI3K also in macrophages, this activity strictly requires TLR2/6 signaling and cannot be mediated by TLR2/1 agonists (Santos-Sierra et al., 2009), such as Pg (Jain et al., 2013). The involvement of PI3K in the evasion of phagocytosis by Pg was an unexpected finding since PI3K is generally thought to promote phagocytic function (Hannigan et al., 2004). However, PI3K activation by high concentrations of C5a (100 nM) leads to inhibition of phagocytosis in neutrophils (Morris et al., 2011). Therefore, high C5a levels, such as those generated by Pg through the enzymatic action of its gingipains (Liang et al., 2011; Wang et al., 2010), could induce altered PI3K signaling that inhibits rather than promotes phagocytosis. Indeed, PI3K signaling activated by Pg-induced C5aR/TLR2 crosstalk inhibited RhoA activation and actin polymerization, thereby accounting for the observed inhibition of phagocytosis (Figure 7).

In the murine periodontal tissue, the capacity of Pg to colonize and mediate dysbiosis required functional C5aR, TLR2, and PI3K, that is, the same key molecules involved in the manipulation of neutrophils (Figure 7), although additional cell types in the periodontal environment express the implicated molecules and might also be affected by Pg. For instance, Pg was shown to activate and exploit PI3K signaling also in gingival epithelial cells, where the pathogen suppresses apoptosis in a PI3K-dependent manner to enhance its intracellular persistence (Yilmaz et al., 2004). Moreover, in co-infection experiments in the chamber model, bystander *F. nucleatum* bacteria acquired resistance to neutrophil killing as long as C5aR, TLR2, and PI3K were all functional. These findings attest to the predictive power of the model proposed (Figure 7).

It is increasingly acknowledged that periodontitis is caused by a synergistic and dysbiotic community of pathobionts rather than by select 'periodontal pathogens' as traditionally thought (Abusleme et al., 2013; Hajishengallis and Lamont, 2012). In such community, the role of Pg is likely to tip the balance from homeostasis to dysbiosis, upon which commensal bacteria can opportunistically mediate destructive inflammation as pathobionts (Hajishengallis, 2014; Jiao et al., 2013). The dissected subversive mechanism of Pg is therapeutically important as it offers potentially promising targets (C5aR, TLR2, Mal, PI3K) for intervention against periodontal dysbiosis and inflammation.

In conclusion, the uncoupling of bacterial clearance from inflammation is a mechanism whereby keystone pathogens can contribute to the persistence of inflammophilic communities that drive dysbiotic inflammatory diseases. In general, the targeting of pathobiotic microbial communities through host modulation therapy is likely to be a more effective strategy to treat polymicrobial inflammatory diseases than traditional direct antimicrobial approaches, especially since mucosal keystone pathogens can act at low levels of abundance (Hajishengallis et al., 2012).

EXPERIMENTAL PROCEDURES

Reagents

All reagents used including mammalian cells, bacterial and mouse strains are described in the *Supplemental Experimental Procedures* together with description of standard techniques (*e.g.*, real-time PCR, siRNA transfection, and immunoprecipitation).

Subcutaneous chamber model

The mouse chamber model was previously described (Burns et al., 2010; Mydel et al., 2006). Briefly, a surgical-grade titanium coil chamber was implanted subcutaneously in the dorsolumbar region of each mouse. After a 7-d healing period, bacteria (10^9 CFU in 0.1-ml PBS) were injected into the chambers with or without inhibitors or control compounds, and the mice were euthanized at different timepoints (2h to 24h post-inoculation). Chamber fluid was aspirated and divided into aliquots that were used for enumeration of recovered CFU (after anaerobic growth on blood agar plates), analysis of recruited cells, and assessment of cytokine responses by ELISA. Kanamycin-Vancomycin blood agar plates were used to grow bacteria in co-infection experiments using *F. nucleatum* (susceptible to kanamycin and resistant to vancomycin) and Pg (resistant to kanamycin and susceptible to vancomycin). All mouse experimental procedures described in this study have been approved by the Institutional Animal Care and Use Committee, in compliance with established federal and state policies.

Killing assay

Neutrophil-Pg suspensions (MOI=1:1) were incubated at 37°C and 5%CO_2 for 2h, at which time the neutrophils were lysed and viable CFU were enumerated after anaerobic culture on blood agar plates. The killing index was calculated according to the formula: [(CFU in the absence of neutrophils–CFU in the presence of neutrophils)/CFU in the absence of neutrophils]×100.

Oxidative burst assay

Neutrophils in glucose-containing HBSS (Life Technologies) were preincubated at 37°C for 15 min with 100 μM 2′,7′-dichlorofluorescin diacetate (Life Technologies) in microtiter culture plates (2×10^5 cells/well). The samples were then incubated with Pg (MOI=1:1) at 37°C for 15 min (Hajishengallis et al., 2008). The fluorescent signal resulting from the oxidation of 2′,7′-dichlorofluorescin into dichlorofluorescein was measured in relative fluorescence units on a microplate fluorescence reader (BioTek) with excitation/emission wavelength settings of 485/530 nm.

Phagocytosis

ATRA-differentiated HL-60 neutrophils were incubated at 37°C with Syto9-labeled Pg (MOI=10:1) for 30 min. After cell washing to remove nonadherent bacteria, extracellular fluorescence (representing attached but not internalized bacteria) was quenched with 0.2% trypan blue. The cells were washed again, fixed, and analyzed by flow cytometry (% positive cells for Syto9-Pg and mean fluorescence intensity). The phagocytic index was calculated using the formula (% positive cells × mean fluorescence intensity)/100. A similar procedure was followed to measure *in vivo* phagocytosis of Pg, in which case Syto9-labeled Pg was injected into the implanted chambers. The chamber contents were harvested 2h post-inoculation for processing and flow cytometry as above.

Bacterial colonization

The levels of Pg colonization and the number of total bacteria in the periodontal tissue were determined using quantitative real-time PCR of the *ISPg1* gene (Pg) and the 16S rRNA gene (total bacteria) (Hajishengallis et al., 2011; McIntosh and Hajishengallis, 2012). Details are given in Supplemental Experimental Procedures.

Cell activation assays

The activation of PI3K (Tyr phosphorylation of p85 subunit) was determined using a colorimetric cell-based ELISA kit (Active Motif). To determine RhoA activation, stimulated neutrophil lysates (10 μg) were subjected to the G-LISA RhoA activation assay (Cytoskeleton). In both assays, the cells were stimulated with Pg (MOI=10:1) for times shown in figure legends.

Actin polymerization

Neutrophils were incubated with Pg (MOI=10:1) for up to 60 min and F-actin levels were determined by phalloidin staining. Specifically, following washing in ice-cold PBS, the cells were fixed with 4% formaldehyde (10 min), permeabilized with 0.1% Triton (5 min), and incubated with rhodamine-conjugated phalloidin (2 μg/ml; 30 min). Rhodamine fluorescence was measured spectrofluometrically.

Fluorescence resonance energy transfer (FRET)

Upon stimulation for 10 min at 37°C with Pg (MOI=10:1), neutrophils were labeled with a mixture of Cy3-conjugated (donor) and Cy5-conjugated (acceptor) antibodies, as indicated in Figure 2E. The cells were washed and fixed, and energy transfer between various donor-

acceptor pairs was calculated from the increase in donor fluorescence after acceptor photobleaching.

Statistical analysis

Data were evaluated by analysis of variance and the Dunnett multiple-comparison test using the InStat program (GraphPad). Where appropriate (comparison of two groups only), two-tailed *t* tests were performed. If SD were significantly different among groups, non-parametric tests were used (Mann-Whitney test for comparison of two groups; Kruskal-Wallis nonparametric ANOVA and multiple comparisons test for comparison of three groups or more). $P < 0.05$ was taken as the level of significance.

Supplementary Material

Refer to Web version on PubMed Central for supplementary material.

Acknowledgments

This work was supported by grants from the National Institutes of Health (AI068730 to J.D.L.; DE015254 and DE021685 to G.H.), the European Commission (FP7-DIREKT 602699 to J.D.L.) and the MRC (UK) (G0900408 to M.A.C.).

REFERENCES

Abe T, Hosur KB, Hajishengallis E, Reis ES, Ricklin D, Lambris JD, Hajishengallis G. Local complement-targeted intervention in periodontitis: proof-of-concept using a C5a receptor (CD88) antagonist. J. Immunol. 2012; 189:5442–5448. [PubMed: 23089394]

Abusleme L, Dupuy AK, Dutzan N, Silva N, Burleson JA, Strausbaugh LD, Gamonal J, Diaz PI. The subgingival microbiome in health and periodontitis and its relationship with community biomass and inflammation. ISME J. 2013; 7:1016–1025. [PubMed: 23303375]

Brzezinska AA, Johnson JL, Munafo DB, Ellis BA, Catz SD. Signalling mechanisms for Toll-like receptor-activated neutrophil exocytosis: key roles for interleukin-1-receptor-associated kinase-4 and phosphatidylinositol 3-kinase but not Toll/IL-1 receptor (TIR) domain-containing adaptor inducing IFNβ (TRIF). Immunology. 2009; 127:386–397. [PubMed: 19019092]

Burns E, Eliyahu T, Uematsu S, Akira S, Nussbaum G. TLR2-dependent inflammatory response to *Porphyromonas gingivalis* is MyD88 independent, whereas MyD88 is required to clear infection. J. Immunol. 2010; 184:1455–1462. [PubMed: 20042569]

Choi CH, Spooner R, DeGuzman J, Koutouzis T, Ojcius DM, Yilmaz O. *Porphyromonas gingivalis*-nucleoside-diphosphate-kinase inhibits ATP-induced reactive-oxygen-species via P2X7 receptor/NADPH-oxidase signalling and contributes to persistence. Cell Microbiol. 2013; 15:961–976. [PubMed: 23241000]

Cyktor JC, Turner J. Interleukin-10 and immunity against prokaryotic and eukaryotic intracellular pathogens. Infect. Immun. 2011; 79:2964–2973. [PubMed: 21576331]

de Haas CJC, Veldkamp KE, Peschel A, Weerkamp F, Van Wamel WJB, Heezius ECJM, Poppelier MJJG, Van Kessel KPM, van Strijp JAG. Chemotaxis inhibitory protein of *Staphylococcus aureus*, a bacterial antiinflammatory agent. J. Exp. Med. 2004; 199:687–695. [PubMed: 14993252]

Eloe-Fadrosh EA, Rasko DA. The human microbiome: from symbiosis to pathogenesis. Annu. Rev. Med. 2013; 64:145–163. [PubMed: 23327521]

Eskan MA, Jotwani R, Abe T, Chmelar J, Lim JH, Liang S, Ciero PA, Krauss JL, Li F, Rauner M, et al. The leukocyte integrin antagonist Del-1 inhibits IL-17-mediated inflammatory bone loss. Nat. Immunol. 2012; 13:465–473. [PubMed: 22447028]

Hajishengallis E, Hajishengallis G. Neutrophil homeostasis and periodontal health in children and adults. J. Dent. Res. 2014; 93:231–237. [PubMed: 24097856]

Hajishengallis G. Immunomicrobial pathogenesis of periodontitis: keystones, pathobionts, and host response. Trends Immunol. 2014; 35:3–11. [PubMed: 24269668]

Hajishengallis G, Darveau RP, Curtis MA. The keystone-pathogen hypothesis. Nat. Rev. Microbiol. 2012; 10:717–725. [PubMed: 22941505]

Hajishengallis G, Lamont RJ. Beyond the red complex and into more complexity: The Polymicrobial Synergy and Dysbiosis (PSD) model of periodontal disease etiology. Mol. Oral Microbiol. 2012; 27:409–419. [PubMed: 23134607]

Hajishengallis G, Lamont RJ. Breaking bad: Manipulation of the host response by *Porphyromonas gingivalis*. Eur. J. Immunol. 2014; 44:328–338. [PubMed: 24338806]

Hajishengallis G, Liang S, Payne MA, Hashim A, Jotwani R, Eskan MA, McIntosh ML, Alsam A, Kirkwood KL, Lambris JD, et al. Low-abundance biofilm species orchestrates inflammatory periodontal disease through the commensal microbiota and complement. Cell Host Microbe. 2011; 10:497–506. [PubMed: 22036469]

Hajishengallis G, Wang M, Bagby GJ, Nelson S. Importance of TLR2 in early innate immune response to acute pulmonary infection with *Porphyromonas gingivalis* in mice. J. Immunol. 2008; 181:4141–4149. [PubMed: 18768871]

Hannigan MO, Huang CK, Wu DQ. Roles of PI3K in neutrophil function. Curr. Top Microbiol. Immunol. 2004; 282:165–175. [PubMed: 14594217]

Hasturk H, Kantarci A, Goguet-Surmenian E, Blackwood A, Andry C, Serhan CN, Van Dyke TE. Resolvin E1 regulates inflammation at the cellular and tissue level and restores tissue homeostasis in vivo. J. Immunol. 2007; 179:7021–7029. [PubMed: 17982093]

Honda F, Kano H, Kanegane H, Nonoyama S, Kim ES, Lee SK, Takagi M, Mizutani S, Morio T. The kinase Btk negatively regulates the production of reactive oxygen species and stimulation-induced apoptosis in human neutrophils. Nat. Immunol. 2012; 13:369–378. [PubMed: 22366891]

Jain S, Coats SR, Chang AM, Darveau RP. A novel class of lipoprotein lipase-sensitive molecules mediates Toll-like receptor 2 activation by *Porphyromonas gingivalis*. Infect. Immun. 2013; 81:1277–1286. [PubMed: 23381996]

Jiao Y, Darzi Y, Tawaratsumida K, Marchesan JT, Hasegawa M, Moon H, Chen GY, Nunez G, Giannobile WV, Raes J, et al. Induction of bone loss by pathobiont-mediated nod1 signaling in the oral cavity. Cell Host Microbe. 2013; 13:595–601. [PubMed: 23684310]

Kagan JC, Medzhitov R. Phosphoinositide-mediated adaptor recruitment controls Toll-like receptor signaling. Cell. 2006; 125:943–955. [PubMed: 16751103]

Lakschevitz FS, Aboodi GM, Glogauer M. Oral neutrophil transcriptome changes result in a pro-survival phenotype in periodontal diseases. PLoS One. 2013; 8:e68983. [PubMed: 23874838]

Lee YS, Park JS, Kim JH, Jung SM, Lee JY, Kim SJ, Park SH. Smad6-specific recruitment of Smurf E3 ligases mediates TGF-beta1-induced degradation of MyD88 in TLR4 signalling. Nat. Commun. 2011; 2:460. [PubMed: 21897371]

Liang S, Krauss JL, Domon H, McIntosh ML, Hosur KB, Qu H, Li F, Tzekou A, Lambris JD, Hajishengallis G. The C5a receptor impairs IL-12-dependent clearance of *Porphyromonas gingivalis* and is required for induction of periodontal bone loss. J. Immunol. 2011; 186:869–877. [PubMed: 21149611]

McIntosh ML, Hajishengallis G. Inhibition of *Porphyromonas gingivalis*-induced periodontal bone loss by CXCR4 antagonist treatment. Mol. Oral Microbiol. 2012; 27:449–457. [PubMed: 23134610]

Miletic AV, Graham DB, Montgrain V, Fujikawa K, Kloeppel T, Brim K, Weaver B, Schreiber R, Xavier R, Swat W. Vav proteins control MyD88-dependent oxidative burst. Blood. 2007; 109:3360–3368. [PubMed: 17158234]

Morris AC, Brittan M, Wilkinson TS, McAuley DF, Antonelli J, McCulloch C, Barr LC, McDonald NA, Dhaliwal K, Jones RO, et al. C5a-mediated neutrophil dysfunction is RhoA-dependent and predicts infection in critically ill patients. Blood. 2011; 117:5178–5188. [PubMed: 21292772]

Moutsopoulos NM, Konkel J, Sarmadi M, Eskan MA, Wild T, Dutzan N, Abusleme L, Zenobia C, Hosur KB, Abe T, et al. Defective neutrophil recruitment in leukocyte adhesion deficiency type I disease causes local IL-17–driven inflammatory bone loss. Sci. Transl. Med. 2014; 6:229ra240.

Mydel P, Takahashi Y, Yumoto H, Sztukowska M, Kubica M, Gibson FC 3rd, Kurtz DM Jr. Travis J, Collins LV, Nguyen KA, et al. Roles of the host oxidative immune response and bacterial antioxidant rubrerythrin during *Porphyromonas gingivalis* infection. PLoS Pathog. 2006; 2:e76. [PubMed: 16895445]

Naiki Y, Michelsen KS, Zhang W, Chen S, Doherty TM, Arditi M. Transforming growth factor-beta differentially inhibits MyD88-dependent, but not TRAM- and TRIF-dependent, lipopolysaccharide-induced TLR4 signaling. J. Biol. Chem. 2005; 280:5491–5495. [PubMed: 15623538]

Nussbaum G, Shapira L. How has neutrophil research improved our understanding of periodontal pathogenesis? J. Clin. Periodontol. 2011; 38:49–59. [PubMed: 21323704]

O'Neill LA, Bowie AG. The family of five: TIR-domain-containing adaptors in Toll-like receptor signalling. Nat. Rev. Immunol. 2007; 7:353–364. [PubMed: 17457343]

Reyes-Robles T, Alonzo F, Kozhaya L, Lacy DB, Unutmaz D, Torres VJ. *Staphylococcus aureus* leukotoxin ED targets the chemokine receptors CXCR1 and CXCR2 to kill leukocytes and promote infection. Cell Host Microbe. 2013; 14:453–459. [PubMed: 24139401]

Rubinstein MR, Wang X, Liu W, Hao Y, Cai G, Han YW. *Fusobacterium nucleatum* promotes colorectal carcinogenesis by modulating E-cadherin/beta-catenin signaling via its FadA adhesin. Cell Host Microbe. 2013; 14:195–206. [PubMed: 23954158]

Ryder MI. Comparison of neutrophil functions in aggressive and chronic periodontitis. Periodontol. 2000. 2010; 53:124–137. [PubMed: 20403109]

Santos-Sierra S, Deshmukh SD, Kalnitski J, Kuenzi P, Wymann MP, Golenbock DT, Henneke P. Mal connects TLR2 to PI3Kinase activation and phagocyte polarization. EMBO J. 2009; 28:2018–2027. [PubMed: 19574958]

Stecher B, Maier L, Hardt WD. 'Blooming' in the gut: how dysbiosis might contribute to pathogen evolution. Nat. Rev. Microbiol. 2013; 11:277–284. [PubMed: 23474681]

Suzuki N, Suzuki S, Duncan GS, Millar DG, Wada T, Mirtsos C, Takada H, Wakeham A, Itie A, Li S, et al. Severe impairment of interleukin-1 and Toll-like receptor signalling in mice lacking IRAK-4. Nature. 2002; 416:750–756. [PubMed: 11923871]

Wahl SM. Transforming growth factor β: the good, the bad, and the ugly. J. Exp. Med. 1994; 180:1587–1590. [PubMed: 7964446]

Wang M, Krauss JL, Domon H, Hosur KB, Liang S, Magotti P, Triantafilou M, Triantafilou K, Lambris JD, Hajishengallis G. Microbial hijacking of complement-toll-like receptor crosstalk. Sci. Signal. 2010; 3:ra11. [PubMed: 20159852]

Wiedemann A, Patel JC, Lim J, Tsun A, van Kooyk Y, Caron E. Two distinct cytoplasmic regions of the β2 integrin chain regulate RhoA function during phagocytosis. J. Cell Biol. 2006; 172:1069–1079. [PubMed: 16567504]

Yang L, Pang Y, Moses HL. TGFβ and immune cells: an important regulatory axis in the tumor microenvironment and progression. Trends Immunol. 2010; 31:220–227. [PubMed: 20538542]

Yilmaz O, Jungas T, Verbeke P, Ojcius DM. Activation of the phosphatidylinositol 3-kinase/Akt pathway contributes to survival of primary epithelial cells infected with the periodontal pathogen *Porphyromonas gingivalis*. Infect. Immun. 2004; 72:3743–3751. [PubMed: 15213114]

HIGHLIGHTS

- *P. gingivalis* degrades MyD88 and interferes with the neutrophil killing function
- *P. gingivalis* activates PI3K which blocks phagocytosis and promotes inflammation
- These mechanisms require crosstalk between complement receptor C5aR and TLR2
- This crosstalk protects *P. gingivalis* and bystander bacteria and promotes dysbiosis

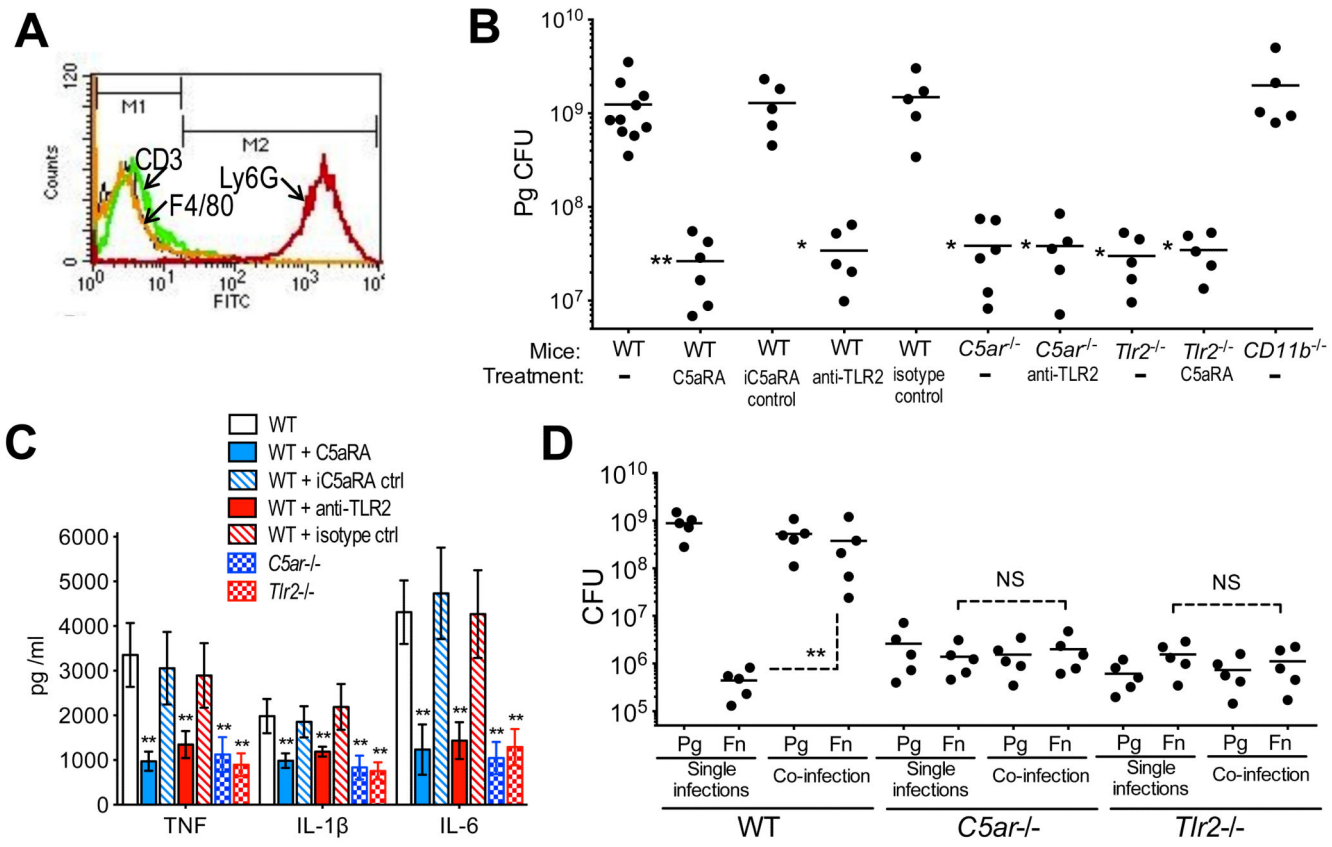

Figure 1. Pg exploits C5aR and TLR2 *in vivo* to inhibit neutrophil killing but not inflammation

(**A**) Pg (10^9 CFU) was injected into implanted chambers in mice and recruited cells were phenotypically characterized by flow cytometry. The majority (>97%) were neutrophils ($Ly6G^+$) whereas macrophages ($F4/80^+$) or T cells ($CD3^+$) were essentially absent. (**B** and **C**) Pg (10^9 CFU) was injected into implanted chambers in WT mice or in the indicated knockout mice (with or without 10 μg C5aRA, iC5aRA control, anti-TLR2, or isotype control). Fluid was aspirated from the chambers 2h post-inoculation and was used to determine viable Pg CFU (**B**) and measure the indicated cytokine responses by ELISA (**C**). Baseline levels (prior to Pg injection) for TNF and IL-1β were undetectable; baseline levels of IL-6 were <10% of the Pg-induced response in WT. (**D**) Pg and *F. nucleatum* (Fn) were injected either alone (10^9 CFU) or together (5×10^8 CFU each) into implanted chambers in WT mice or in the indicated knockout mice. At 24h post-inoculation, chamber fluid was aspirated to determine viable CFU. In **B** and **D**, each symbol represents an individual mouse and horizontal lines indicate means. In **C**, data are means ± SD (*n*=5-6 mice per group except for WT; *n*=10 mice). The experiments were performed twice yielding consistent results. **P*<0.05 and ***P*<0.01 compared with untreated WT control (**B** and **C**) or between the indicated groups (**D**). NS, not significant. See also Figure S1.

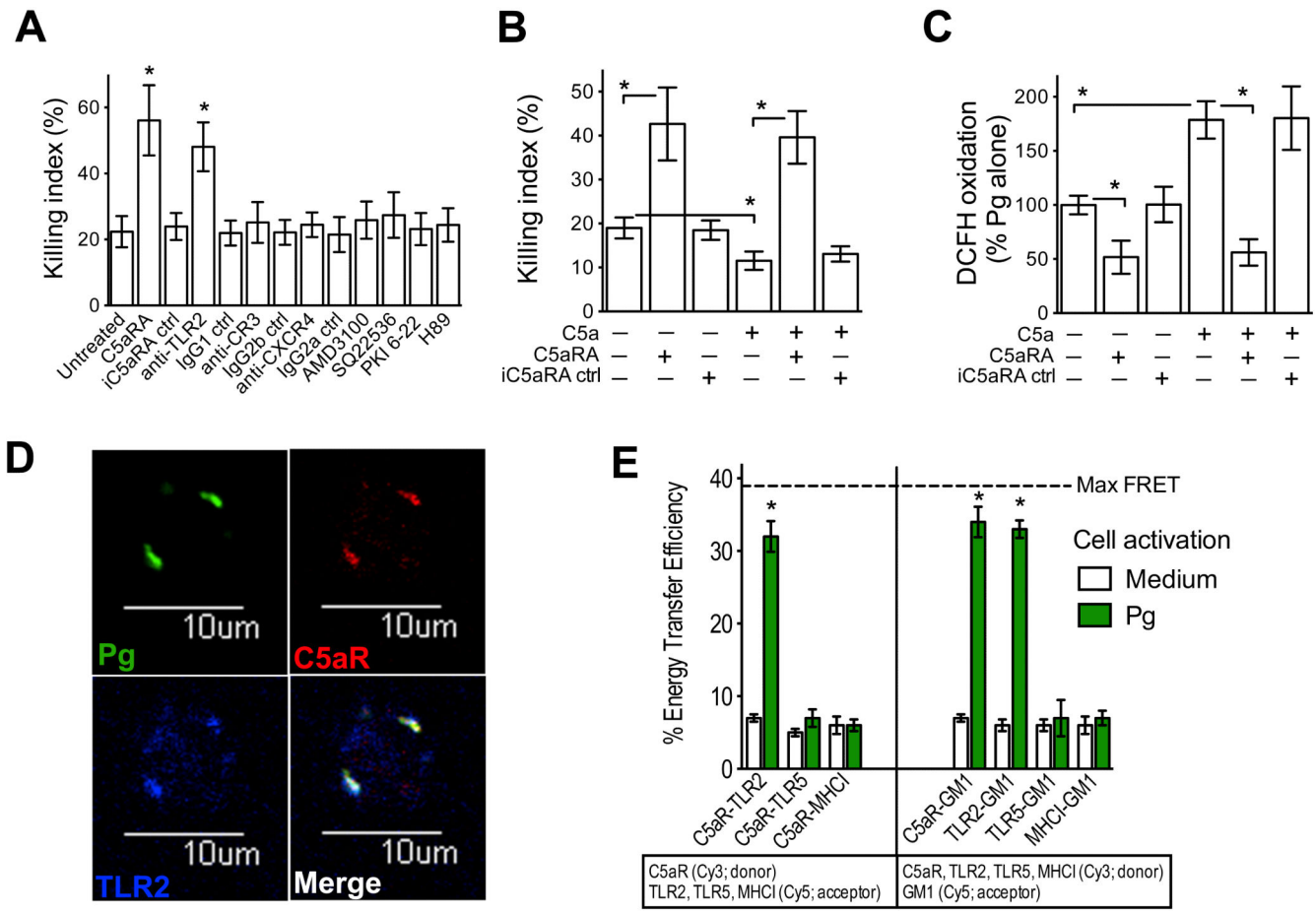

Figure 2. Interactions of Pg with human neutrophils

(**A-C**) *In vitro* killing (**A, B**) and oxidative burst (**C**) assays using purified human neutrophils and Pg in the presence of the indicated compounds. In **A**, mAbs to TLR2, CR3, CXCR4, and isotype controls were used at 10 μg/ml; AMD3100, 1 μg/ml; C5aRA and iC5aRA control, each at 1 μM; SQ22536, 200 μM; PKI 6-22, 1 μM; and H-89, 10 μM. In **B** and **C** exogenous C5a was added at 10 nM, whereas C5aRA and iC5aRA control were each added at 1 μM. (**D** and **E**) Neutrophil activation by Pg induces C5aR-TLR2 co-association. (**D**) Human neutrophils were challenged with Syto9-labeled Pg (green) for 30 min (MOI=10:1) followed by fixation and staining for C5aR (red) and TLR2 (blue). Bottom right, merged image. (**E**) Human neutrophils were challenged with Pg (MOI=10:1) for 10 min. FRET between the indicated donors and acceptors was measured from the increase in donor (Cy3) fluorescence after acceptor (Cy5) photobleaching. All data are means ± SD (*n* =3) from one of at least two experiments yielding similar results. The horizontal dashed line indicates the maximum (max) energy transfer efficiency in the experimental system determined as the energy transfer between two different epitopes on the same molecule (C5aR). **P*<0.01 compared with untreated control (medium only) or between the indicated groups.

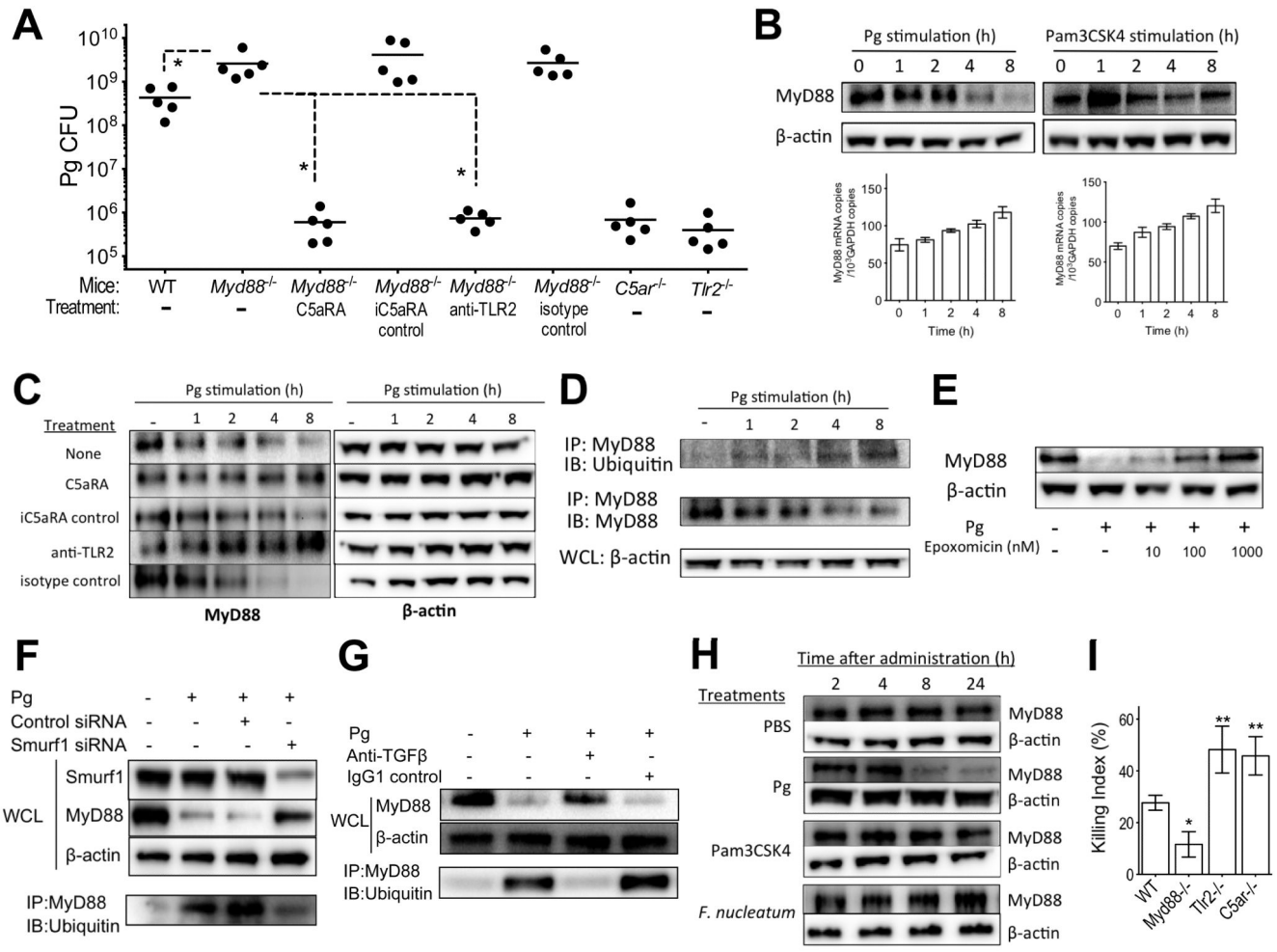

Figure 3. Pg causes a reduction in the levels of MyD88, which promotes bacterial killing

(**A**) Pg (10^9 CFU) was injected into implanted chambers in WT mice or in the indicated knockout mice (with or without 10 μg C5aRA, iC5aRA control, anti-TLR2, or isotype control). Fluid was aspirated from the chambers 24h post-inoculation and was used to determine viable Pg CFU. (**B**-**E**) Pg was incubated *in vitro* with human neutrophils (MOI=10:1) for the indicated times and immunoblotting of neutrophil lysates was used to monitor the levels of MyD88 protein (or β-actin; control). In **B**, Pg was compared with Pam3CSK4 (10 ng/ml) and their effects on MyD88 were monitored also at the mRNA level using real-time PCR. In **C**, neutrophils were stimulated with Pg in the presence of C5aRA or iC5aRA control (each at 1 μM) or anti-TLR2 mAb or isotype control (10 μg/ml). In **D**, cell lysates immunoprecipitated using anti-MyD88 were probed with antibodies to MyD88 or to ubiquitin. In **E**, neutrophils were stimulated with Pg in the presence of increasing concentrations of epoxomycin. (**F**) ATRA–HL-60 neutrophils were transfected with siRNA to Smurf1 and treated with Pg (MOI=10:1) for 8h. Whole cell-lysate immunoblotting with specific antibodies was used to monitor the levels of Smurf1 and MyD88 protein (β-actin was used as control). Cell lysates immunoprecipitated using anti-MyD88 were immunoblotted with anti-ubiquitin. (**G**) Human neutrophils were treated with Pg and assayed for MyD88 degradation and ubiquitination as in **F** in the absence or presence of

anti-TGF-β mAb. (**H**) The indicated bacteria or compounds were injected (Pg, 10^9 CFU; Pam3SK4, 10 μg; *F. nucleatum*, 10^9 CFU) into implanted chambers in mice for the indicated times and immunoblotting of neutrophil lysates was used to monitor the levels of MyD88 protein. (**I**) Assay for *in vitro* killing of Pg by purified mouse neutrophils of the indicated genotypes. All experiments were performed two (**A**) or three times (**B-I**) yielding similar findings. In **A**, each symbol represents an individual mouse and horizontal lines indicate means. In **I**, data are means ± SD (n=4). *P<0.05 and **P<0.01 compared with WT control or between the indicated groups. IB, immunoblotting; IP, immunoprecipitation; WCL, whole cell lysates. See also Figure S2.

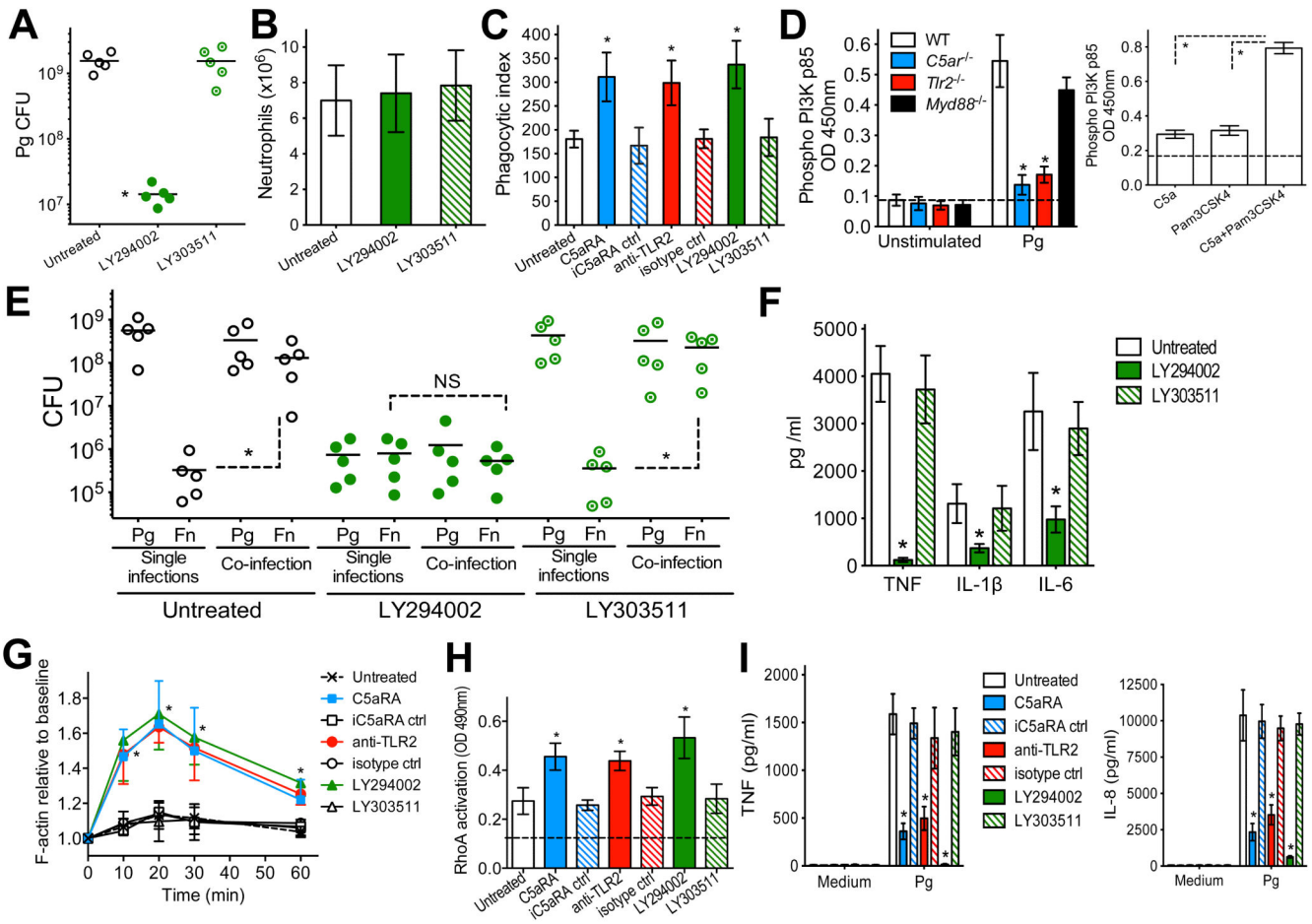

Figure 4. PI3K promotes inflammation and the survival of Pg by inhibiting its phagocytosis *in vivo*

(**A-C**) Pg (10^9 CFU) was injected into implanted chambers in WT mice, with or without 10 μg LY294002 (PI3K inhibitor) or LY303511 (control). Fluid aspirated from the chambers 2h post-inoculation was used to determine viable Pg CFU (**A**), neutrophil recruitment (**B**), and Pg phagocytosis (**C**). In C, the experiment additionally included treatments with C5aRA, anti-TLR2, and respective controls (all at 10 μg). (**D**) Activation of PI3K in mouse neutrophils after 15-min-stimulation with Pg (left) or with 10 nM C5a and/or 100 ng/ml Pam3CSK4 (right) using FACE PI3Kp85 ELISA. In the left panel, neutrophils were from WT or indicated knockout mice. (**E**) Pg and *F. nucleatum* (Fn) were injected either alone (10^9 CFU) or together (5×10^8 CFU each) into implanted chambers in WT mice with or without 10 μg LY294002 or LY303511. At 24h post-inoculation, chamber fluid was aspirated to determine viable CFU. (**F**) Fluid aspirated from chambers 2h post-inoculation with Pg was used to measure the indicated cytokine responses by ELISA. (**G**) Changes in polymerized F-actin over time in human neutrophils exposed to Pg (MOI=10:1) and treated with or without C5aRA or iC5aRA control (1 μM), anti-TLR2 mAb or isotype control (10μg/ml), LY294002 or LY303511 (25 μM). Results are expressed as fold change relative to F-actin at baseline set as 1. (**H**) Human neutrophils were treated as in **G** and after 20-min stimulation with Pg the activation of RhoA was determined using the G-LISA RhoA assay

kit. The dashed line indicates baseline RhoA activation (in cells not exposed to Pg). (**I**) Human neutrophils were treated as in **G** and after 6h-stimulation with Pg the indicated cytokine responses were measured by ELISA. In **A** and **E**, each symbol represents an individual mouse and horizontal lines indicate means. In bar graphs, data are means ± SD (**B**, **C**, and **F**, *n*=5; **D** and **G-I**, *n*=3). The experiments were performed two (**A-C** and **E-H**) or three times (**D,I**) yielding consistent results. **P* <0.01 compared with control (WT or untreated) or between the indicated groups. NS, not significant. See also Figure S3.

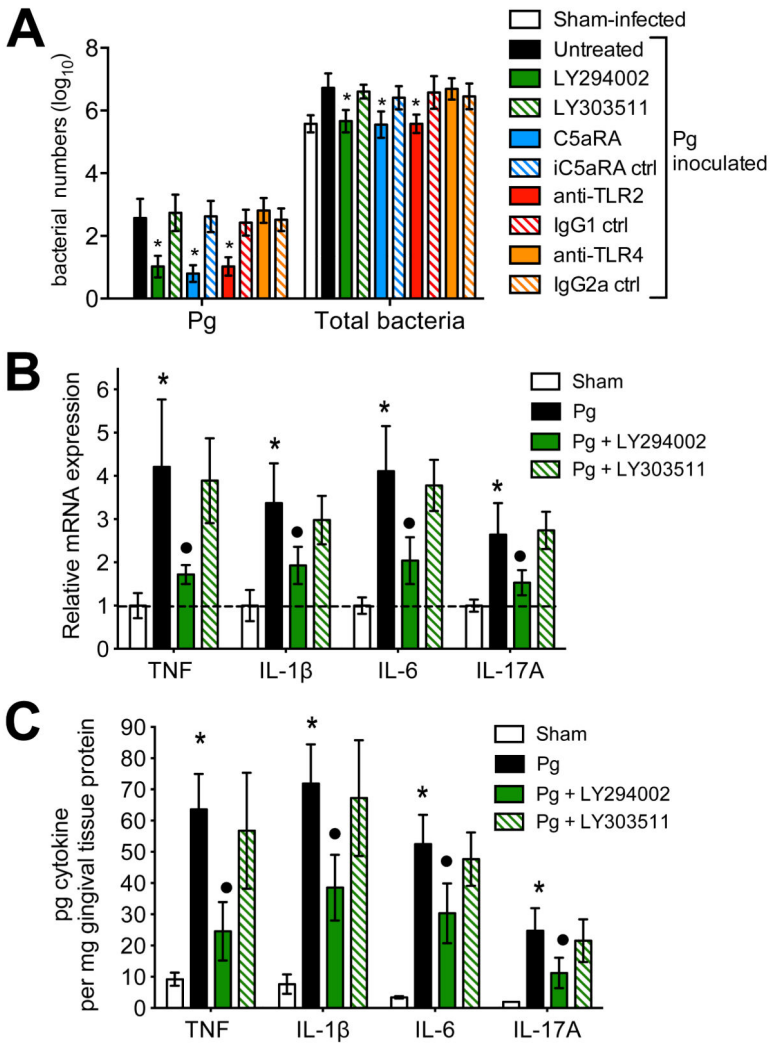

Figure 5. PI3K promotes dysbiotic inflammation in the periodontal tissue

Mice were orally inoculated or not with Pg (10^9 CFU; three times at 2-day intervals) and seven days after the last inoculation were injected with the indicated experimental or control compounds into the palatal gingiva, on the mesial of the first molar and in the papillae between first and second and third molars on both sides of the maxilla (1 μl of 1 μg per site; total of 6 μg in six sites). Two days later, the mice were euthanized and maxillary periodontal tissue was harvested to determine Pg and total bacterial numbers using real-time PCR (**A**) or was used to measure the indicated cytokine responses at the mRNA (**B**) or protein (**C**) level. The mRNA expression levels were normalized against GAPDH mRNA and expressed as fold induction relative to the transcript levels of sham-infected mice, which were assigned an average value of 1. Data are means ± SD (*n*=5 mice) from one of two experiments yielding consistent results. **P*<0.01 compared with untreated control (**A**) or with sham control (**B**, **C**); •*P*<0.01 compared with Pg alone. No Pg could be detected in sham-infected mice. See also Figure S4.

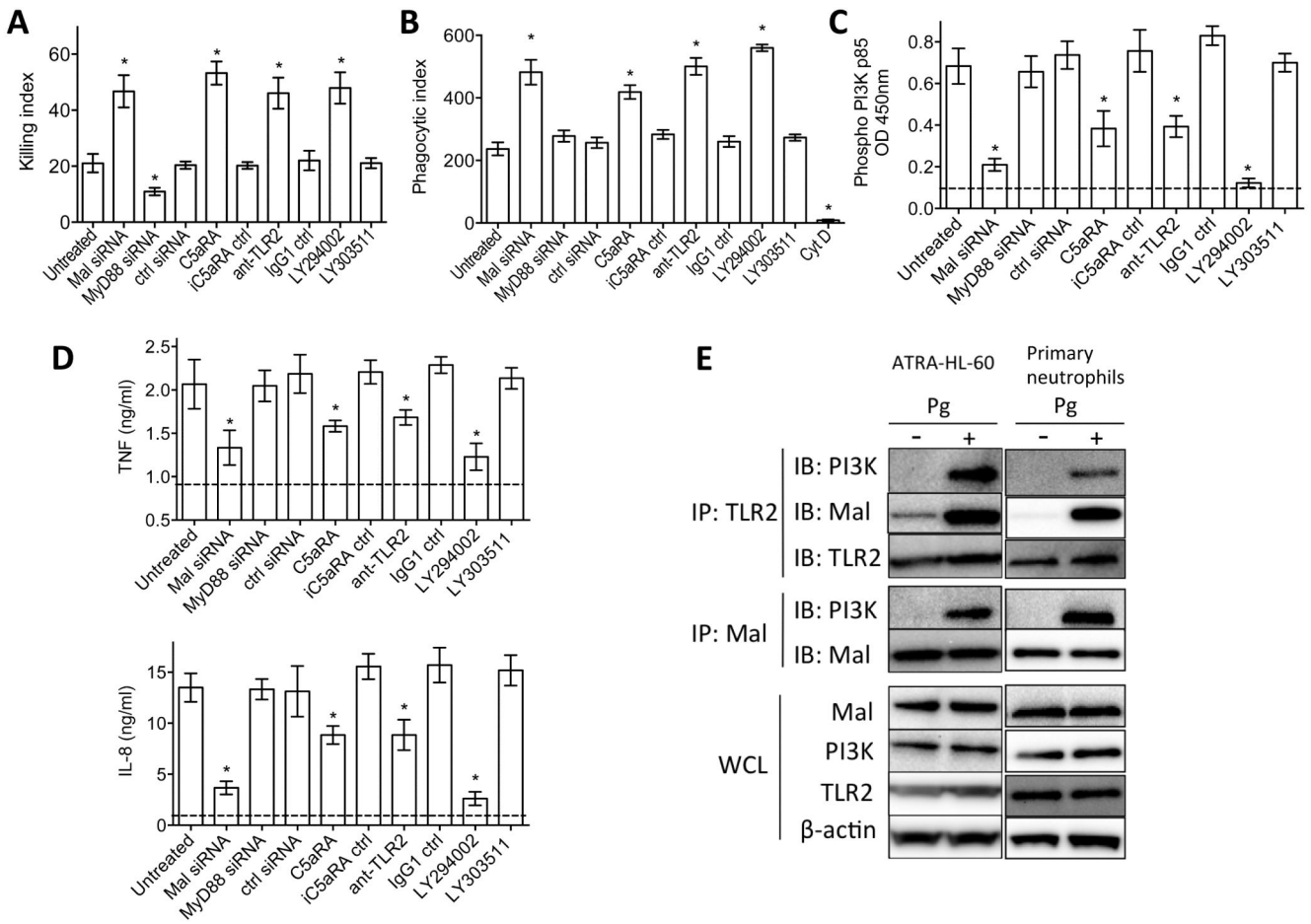

Figure 6. Mal is a component of the C5aR-TLR2 subversive pathway acting upstream of PI3K

(**A-D**) ATRA-differentiated HL-60 neutrophils were transiently transfected with control siRNA or siRNA to Mal or MyD88 (all at 40 nM), or were treated with the indicated compounds (LY294002 or LY303511, 25 μM; C5aRA or iC5aRA control, 1 μM; anti-TLR2 mAb or isotype control, 10μg/ml). The cells were used in assays of Pg killing (**A**) and phagocytosis (**B**) or in assays of PI3K activation (**C**) and cytokine release (**D**). In **B**, cytochalasin D (CytD) was used as negative control for phagocytosis. In **C** and **D**, the horizontal dashed lines indicate baseline levels of PI3K activation and cytokines determined on unstimulated cells. (**E**) Pg-stimulated lysates of ATRA-differentiated HL-60 or primary neutrophils were immunoprecipitated with antibodies to TLR2 or Mal and were probed with antibodies to PI3K, Mal, and TLR2. Pg stimulation was carried out at a MOI equal to 10:1 and for 15 min. Data are means ± SD (**A** and **D**, *n*=5; **B** and **C**, *n* =3). All experiments were performed two times or more yielding similar results. **P*<0.01 compared with untreated control. IB, immunoblotting; IP, immunoprecipitation; WCL, whole cell lysates. See also Figure S5.

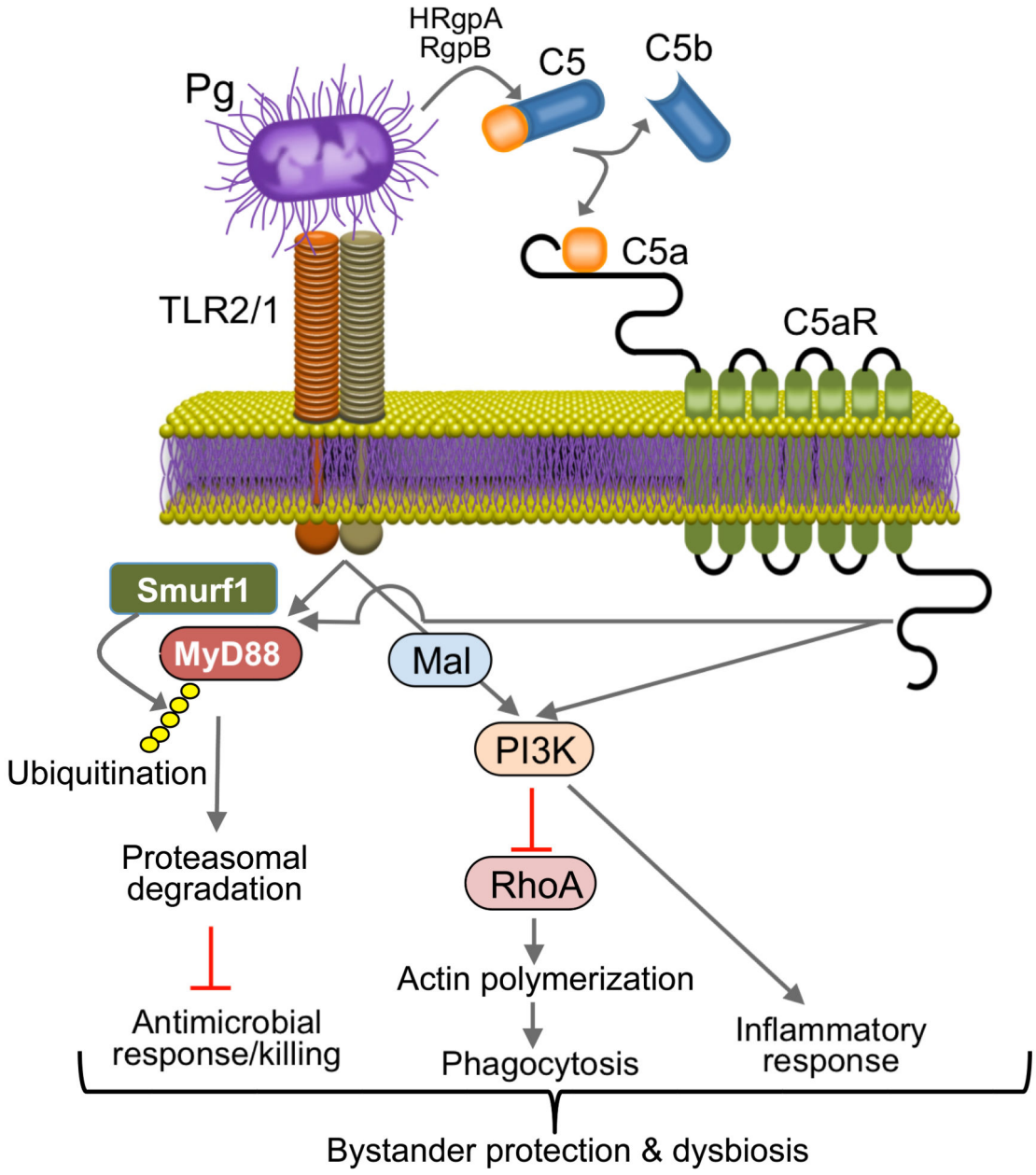

Figure 7. Model of Pg subversion of neutrophils leading to dysbiotic inflammation

Pg co-activates TLR2 and C5aR in neutrophils and the resulting crosstalk leads to ubiquitination and proteasomal degradation of MyD88, thereby inhibiting a host-protective antimicrobial response. This activity requires C5aR/TLR2-dependent release of TGF-β1 (Figure S2J), which mediates ubiquitin-proteasome degradation of MyD88 via the E3 ubiquitin ligase Smurf1. Moreover, the C5aR-TLR2 crosstalk activates PI3K, which prevents phagocytosis through inhibition of RhoA activation and actin polymerization, while stimulating an inflammatory response. In contrast to MyD88, Mal is a component of the subversive pathway acting upstream of PI3K. The integrated mechanism provides

'bystander' protection to otherwise susceptible bacterial species and promotes polymicrobial dysbiotic inflammation *in vivo*.